PRICING AND HEDGING OF QUANTILE OPTIONS IN A FLEXIBLE JUMP DIFFUSION MODEL

NING CAI,* *The Hong Kong University of Science and Technology*

Abstract

This paper proposes a Laplace-transform-based approach to price the fixed-strike quantile options as well as to calculate the associated hedging parameters (delta and gamma) under a hyperexponential jump diffusion model, which can be viewed as a generalization of the well-known Black–Scholes model and Kou's double exponential jump diffusion model. By establishing a relationship between floating- and fixed-strike quantile option prices, we can also apply this pricing and hedging method to floating-strike quantile options. Numerical experiments demonstrate that our pricing and hedging method is fast, stable, and accurate.

Keywords: Jump diffusion; option pricing; hyperexponential; quantile option; Euler inversion

2010 Mathematics Subject Classification: Primary 60J75
Secondary 44A10

1. Introduction

A quantile option is a fairly new path-dependent security derivative that was first introduced by Miura [28]. It has a payoff dependent on the α-quantile, for some $\alpha \in [0, 1]$, of the underlying asset price process during a prespecified time period $[0, T]$, which is defined as the smallest barrier such that the fraction of time spent by the underlying price at or below it during $[0, T]$ exceeds α (see Definition 2.1). Since their advent, quantile options have received much attention from both investors and researchers primarily because they may be regarded as an alternative of many popular exotic options such as barrier, lookback, and Asian options. First, as discussed by Broadie and Detemple [6], a fixed-strike quantile option may serve as a replacement for the standard Barrier option by overcoming its deficiency of leaving the buyer without his or her position at the first cross of the barrier. Second, a floating-strike α-quantile put option extends the traditional lookback put option by replacing the running maximum of the underlying asset price process in the payoff with its α-quantile. Apparently, the former is reduced to the latter as $\alpha = 1$. Third, a special α-quantile option when $\alpha = 0.5$ behaves similarly to the Asian option due to the close relationship between the median and the mean.

Under the Black–Scholes model (BSM), distributions of the associated quantiles have been studied by Dassios [13] (also see [4], [17], and [34]) and led to analytical solutions to pricing of the fixed-strike quantile options; see [2] and [13]. Leung and Kwok [26] established a relationship between fixed- and floating-strike quantile option prices under the BSM. However, as regards numerical implementation, few papers offer numerical results even under the BSM due to computational intractability of available pricing formulae, which involve multiple integrals. One example is the forward shooting grid method developed by Kwok and Lau [25]. For pricing other options dependent on quantiles or occupation times under the BSM, we refer

the reader to, e.g. [15], [18], [19], [21], [27], and [29]. In terms of the literature of quantile option pricing beyond the BSM, see, e.g. the occupation time-based approach in [26] under the constant elasticity of variance (CEV) model and in [9] under Kou's double exponential jump diffusion model (abbreviated to DEM).

In this paper we will investigate pricing and hedging of both fixed- and floating-strike quantile options under a hyperexponential jump diffusion model (abbreviated to HEM) (see, e.g. [8] and [22]), where the jump sizes assume a hyperexponential distribution. As a generalization of the BSM and DEM, the HEM has at least three advantages. First, it can better capture the leptokurtic feature by accounting for the uncertainty about heaviness of asset return tails. Second, it can be used to approximate exponential Lévy models with completely monotone Lévy densities such as the CGMY, NIG, and VG models. Third, it can lead to analytical solutions of many path-dependent options such as lookback, single-barrier, and double-barrier options. In this paper it will be shown that we can also price quantile options and calculate the hedging parameters thanks to the analytical tractability of the HEM.

The contribution of our paper is three-fold.

1. Based on Dassios' remarkable identity in law on quantiles of Lévy processes (see [14]), we develop a Laplace-transform-based method to price the fixed-strike quantile option and to calculate the hedging parameters (delta and gamma) numerically under the HEM. See Section 3.1.

2. By establishing a simple relationship between floating- and fixed-strike quantile option prices under the HEM, we can also price floating-strike quantile options and calculate the hedging parameters in a similar way. See Section 3.2.

3. We implement the pricing and hedging methods by using the Euler inversion algorithm twice. The primary difficulty lies in the fact that in general the Euler inversion algorithm applies only for real original functions, but during the implementation we need to evaluate a complex function by inverting its Laplace transform. We circumvent this difficulty by evaluating the real part and the imaginary part of the complex function by inverting their respective Laplace transforms. See Section 4.2. This numerical pricing method turns out to be fast, stable, and accurate. See Section 5. In particular, under the BSM, this method can be simplified to a single Euler inversion in that in this special case, a closed-form Laplace transform of the quantile option price is available. See Section 3.1.

The rest of the paper is organized as follows. Section 2 introduces the HEM and some preliminaries. In Section 3 we present our main results, including pricing and hedging of the fixed-strike quantile options, and establishing a relationship between floating- and fixed-strike quantile option prices. In Section 4, a pricing and hedging algorithm based on Euler inversion is discussed in detail. Numerical results are provided in Section 5. Most proofs are deferred to Appendices A and B.

2. Background and preliminaries

2.1. The HEM

Under the HEM, for the asset price $S(t)$, the return process $X(t) := \log(S(t)/S(0))$ under a risk-neutral probability measure P is given by

$$X(t) = \mu t + \sigma W(t) + \sum_{i=1}^{N(t)} Y_i, \qquad X(0) = 0. \tag{2.1}$$

Here $\mu = r - \sigma^2/2 - \lambda\zeta$, $\zeta = \mathrm{E}[e^{Y_1}] - 1$, r is the risk-free interest rate, σ is the volatility, $\{N(t): t \geq 0\}$ is a Poisson process with rate λ, $\{W(t): t \geq 0\}$ is a standard Brownian motion, and $\{Y_i: i = 1, 2, \ldots\}$ is a sequence of independent, identically distributed (i.i.d.) hyperexponential random variables with probability density function (PDF)

$$f_Y(x) = \sum_{i=1}^{m} p_i \eta_i e^{-\eta_i x} \mathbf{1}_{\{x \geq 0\}} + \sum_{j=1}^{n} q_j \theta_j e^{\theta_j x} \mathbf{1}_{\{x < 0\}}, \tag{2.2}$$

where $p_i > 0$ and $\eta_i > 1$ for all $i = 1, \ldots, m$, $q_j > 0$ and $\theta_j > 1$ for all $j = 1, \ldots, n$, and $\sum_{i=1}^{m} p_i + \sum_{j=1}^{n} q_j = 1$. Here $\eta_i > 1$ for all i and $\theta_j > 1$ for all j guarantee finiteness of both $\mathrm{E}[e^{Y_1}]$ and $\mathrm{E}[e^{-Y_1}]$. Moreover, it is assumed that $\{N(t)\}$, $\{W(t)\}$, and $\{Y_i\}_{i=1}^{\infty}$ are independent.

We point out that the risk-neutral probability measure P is not unique within the jump diffusion framework due to the incompleteness of the model. However, Kou [23] showed that a particular risk-neutral probability measure P can be chosen within a rational expectations equilibrium setting. It is called risk neutral because the equilibrium price is given by the expectation under P of the discounted option payoff.

Note that $\{X(t)\}$ is a Lévy process and its Lévy exponent is given by

$$G(x) := \frac{\log(\mathrm{E}[e^{xX(t)}])}{t} = \frac{\sigma^2}{2} x^2 + \mu x + \lambda \left(\sum_{i=1}^{m} \frac{p_i \eta_i}{\eta_i - x} + \sum_{j=1}^{n} \frac{q_j \theta_j}{\theta_j + x} - 1 \right).$$

It can be easily shown (see, e.g. [7]) that the equation $G(x) = s$ for all $s > 0$ has exactly $m + n + 2$ real roots $\beta_{1,s}, \beta_{2,s}, \ldots, \beta_{m+1,s}, \gamma_{1,s}, \gamma_{2,s}, \ldots, \gamma_{n+1,s}$ that satisfy

$$-\infty < \gamma_{n+1,s} < -\theta_n < \gamma_{n,s} < -\theta_{n-1} < \cdots < \gamma_{2,s} < -\theta_1 < \gamma_{1,s} < 0,$$
$$0 < \beta_{1,s} < \eta_1 < \beta_{2,s} < \cdots < \eta_{m-1} < \beta_{m,s} < \eta_m < \beta_{m+1,s} < +\infty. \tag{2.3}$$

These roots will be used in the subsequent parts.

2.2. Running maxima and running minima

Consider the running maximum and running minimum of the process $\mathcal{X} := \{X(t)\}$:

$$M_{\mathcal{X}}(t) := \sup_{\{0 \leq s \leq t\}} X(s) \quad \text{and} \quad m_{\mathcal{X}}(t) := \inf_{\{0 \leq s \leq t\}} X(s).$$

Denote by $\mathcal{L}_M(s)$ and $\mathcal{L}_m(s)$ the Laplace transforms of $\mathrm{E}[e^{vM_{\mathcal{X}}(t)}]$ and $\mathrm{E}[e^{vm_{\mathcal{X}}(t)}]$ with respect to (w.r.t.) t, respectively. More precisely,

$$\mathcal{L}_M(s) := \int_0^{\infty} e^{-st} \mathrm{E}[e^{vM_{\mathcal{X}}(t)}] \, dt \quad \text{and} \quad \mathcal{L}_m(s) := \int_0^{\infty} e^{-st} \mathrm{E}[e^{vm_{\mathcal{X}}(t)}] \, dt.$$

Under the HEM, Cai and Kou [8] derived a closed-form expression of $\mathcal{L}_M(s)$ by connecting it with the first passage time distribution. For convenience, we present this result in Proposition 2.1.

Proposition 2.1. *For any $v \in (-\infty, \beta_1)$, we have*

$$\mathcal{L}_M(s) = \frac{1}{s} + \frac{v}{s} \sum_{l=1}^{m+1} \frac{d_l}{\beta_l - v}, \qquad s > 0,$$

where $\beta_1, \beta_2, \ldots, \beta_{m+1}$, namely $\beta_{1,s}, \beta_{2,s}, \ldots, \beta_{m+1,s}$ given in (2.1), are the $m + 1$ positive roots of the equation $G(x) = s$ and $d := (d_1, d_2, \ldots, d_{m+1})^\top$ is uniquely determined by the linear system $Ad = I$, where $I = (1, 1, \ldots, 1)^\top$ is an $(m+1)$-dimensional unit vector and A is the $(m + 1) \times (m + 1)$ nonsingular matrix

$$
A = \begin{pmatrix}
1 & 1 & \cdots & 1 \\
\dfrac{\eta_1}{\eta_1 - \beta_1} & \dfrac{\eta_1}{\eta_1 - \beta_2} & \cdots & \dfrac{\eta_1}{\eta_1 - \beta_{m+1}} \\
\dfrac{\eta_2}{\eta_2 - \beta_1} & \dfrac{\eta_2}{\eta_2 - \beta_2} & \cdots & \dfrac{\eta_2}{\eta_2 - \beta_{m+1}} \\
\vdots & \vdots & \ddots & \vdots \\
\dfrac{\eta_m}{\eta_m - \beta_1} & \dfrac{\eta_m}{\eta_m - \beta_2} & \cdots & \dfrac{\eta_m}{\eta_m - \beta_{m+1}}
\end{pmatrix}.
$$

Noting that $m_{\mathcal{X}}(t) = \inf_{\{0 \le s \le t\}} X(s) = -\sup_{\{0 \le s \le t\}}(-X(s))$ and applying Proposition 2.1, we can also derive a closed-form expression for $\mathcal{L}_m(s)$.

Remark 2.1. We point out that using the Wiener–Hopf factorization (see, e.g. [3]), we can express $\mathcal{L}_M(s)$ (or $\mathcal{L}_m(s)$) in another way as products of some terms:

$$
\mathcal{L}_M(s) = \frac{1}{s} \frac{\prod_{i=1}^{m+1}(-\beta_i) \prod_{i=1}^{m}(\eta_i - v)}{\prod_{i=1}^{m} \eta_i \prod_{i=1}^{m+1}(v - \beta_i)}.
$$

2.3. Quantile options

The α-quantile of the process $\mathcal{X}$ during the period $[0, t]$ can be defined through the occupation time.

Definition 2.1. Let $\Gamma(x, t, \mathcal{X}) := \int_0^t \mathbf{1}_{\{X(s) \le x\}} \, ds$ represent the occupation time of the process $\mathcal{X} := \{X(s) : s \ge 0\}$ staying below a fixed barrier x during the period $[0, t]$. Then, for any $\alpha \in [0, 1]$, the α-quantile of the process $\mathcal{X}$ during the period $[0, t]$ is defined as

$$
Q(\alpha, t, \mathcal{X}) := \inf \left\{ x : \frac{\Gamma(x, t, \mathcal{X})}{t} > \alpha \right\}.
$$

Then, under the risk neutral measure P, the prices of fixed- and floating-strike α-quantile options at time 0 with maturity t are given by

$$
C_\alpha(S_0, K, t) = e^{-rt} E[(S_0 e^{Q(\alpha, t, \mathcal{X})} - K)^+]
$$

and

$$
P_\alpha(S_0, t) = e^{-rt} E[(S_0 e^{Q(\alpha, t, \mathcal{X})} - S_t)^+],
$$

respectively. For asset pricing theories, we refer the reader to [24] and [33].

Apparently, the distribution of the α-quantile plays a pivotal role for pricing of α-quantile options. Dassios [14] provided a remarkable result about the quantile distribution for any process with stationary and independent increments.

Proposition 2.2. ([14].) *Suppose that* $\{X(t) : t \geq 0\}$ *is a process with stationary and independent increments which starts from* 0. *Then, for any* $\alpha \in (0, 1)$,

$$Q(\alpha, t) \stackrel{D}{=} \sup_{\{0 \leq s \leq \alpha t\}} X^{(1)}(s) + \inf_{\{0 \leq s \leq (1-\alpha)t\}} X^{(2)}(s), \tag{2.4}$$

where $\{X^{(1)}(s) \colon s \geq 0\}$ *and* $\{X^{(2)}(s) \colon s \geq 0\}$ *are independent copies of the process* $\{X(s) \colon s \geq 0\}$.

This celebrated result is useful as it applies to any Lévy process and, hence, also applies to the return process under the HEM. Dassios' result (2.4) will serve as a basis for our approach to pricing and hedging fixed-strike quantile options in the subsequent sections.

3. Pricing and hedging of quantile options

3.1. Pricing and hedging of fixed-strike quantile options

To price and hedge a fixed-strike quantile option, applying the idea of Carr and Madan [10], we consider taking the Laplace transform of the option price w.r.t. $\bar{k} := -\log K$. Since $\bar{k}$ can be negative, the associated Laplace transform is a two-sided Laplace transform, meaning that the original function is defined on the whole real line. In order to apply the two-sided Euler inversion algorithm proposed by Petrella [30], we introduce a scaling factor $X > S_0$ and rewrite the fixed-strike quantile option price as

$$C_\alpha(S_0, K, t) = \mathrm{e}^{-rt} C_\alpha^*(S_0, k, t) \quad \text{with} \quad C_\alpha^*(S_0, k, t) := X \, \mathrm{E}\left[\left(\frac{S_0}{X} \mathrm{e}^{Q(\alpha, t, \mathcal{X})} - \mathrm{e}^{-k} \right)^+ \right],$$

where $k := \log(X/K)$. Here the introduction of the scaling factor X ensures that the Euler Laplace inversion algorithm converges quickly in the two-sided case (see [30]).

Denote by $\mathcal{L}(v)$ the Laplace transform of $C_\alpha^*(S_0, k, t)$ w.r.t. k. More precisely,

$$\mathcal{L}(v) = \int_{-\infty}^{+\infty} \mathrm{e}^{-vk} C_\alpha^*(S_0, k, t) \, \mathrm{d}k = \int_{-\infty}^{+\infty} \mathrm{e}^{-vk} X \, \mathrm{E}\left[\left(\frac{S_0}{X} \mathrm{e}^{Q(\alpha, t, \mathcal{X})} - \mathrm{e}^{-k} \right)^+ \right] \mathrm{d}k.$$

According to Proposition 2.2, we can obtain the following theorem.

Theorem 3.1. (Pricing and hedging of fixed-strike quantile options.) *For any* $v > 0$, *we have*

$$\mathcal{L}(v) = \frac{S_0^{v+1}}{v(v+1)X^v} \, \mathrm{E}[\mathrm{e}^{(v+1)M_X(\alpha t)}] \mathrm{E}[\mathrm{e}^{(v+1)m_X((1-\alpha)t)}]. \tag{3.1}$$

In particular, under the BSM, $\mathcal{L}(v)$ *has the closed-form expression*

$$\mathcal{L}(v) = \frac{S_0^{v+1}}{v(v+1)X^v} h(v+1; \mu, \alpha t) h(-v-1; -\mu, (1-\alpha)t), \tag{3.2}$$

where

$$h(v; \mu, t) := \frac{v\sigma^2 + \mu}{v\sigma^2 + 2\mu} \exp\left(\frac{v\sigma^2 t}{2v\sigma^2 + 4\mu} \right) \mathrm{Erfc}\left(-\frac{(v\sigma^2 + \mu)\sqrt{t}}{\sigma\sqrt{2}} \right)$$
$$+ \frac{\mu}{v\sigma^2 + 2\mu} \mathrm{Erfc}\left(\frac{\mu\sqrt{t}}{\sigma\sqrt{2}} \right),$$

and $\mathrm{Erfc}(z) := (2/\sqrt{\pi}) \int_z^{+\infty} \mathrm{e}^{-x^2} \, \mathrm{d}x$ *represents the complementary error function.*

The two common Greeks $\Delta(C_\alpha(S_0, K, t))$ *and* $\Gamma(C_\alpha(S_0, K, t))$ *can be calculated as*

$$\Delta(C_\alpha(S_0, K, t)) = \frac{\partial}{\partial S_0} C_\alpha(S_0, K, t) = \mathrm{e}^{-rt} \mathcal{L}^{-1}\left(\frac{(v+1)\mathcal{L}(v)}{S_0}\right)\Bigg|_{k=\ln(X/K)},$$

$$\Gamma(C_\alpha(S_0, K, t)) = \frac{\partial^2}{\partial S_0^2} C_\alpha(S_0, K, t) = \mathrm{e}^{-rt} \mathcal{L}^{-1}\left(\frac{v(v+1)\mathcal{L}(v)}{S_0^2}\right)\Bigg|_{k=\ln(X/K)},$$

where $\mathcal{L}^{-1}$ *denotes the inverse Laplace transform.*

Proof. See Appendix A.

Consequently, under the BSM the closed-form Laplace transform $\mathcal{L}(v)$ is available, so applying the Euler inversion algorithm can generate numerical prices and the two Greeks easily. In contrast, under the general HEM, Theorem 3.1 does not provide us with a closed-form Laplace transform $\mathcal{L}(v)$ because neither $\mathrm{E}[\mathrm{e}^{(v+1)M_X(\alpha t)}]$ nor $\mathrm{E}[\mathrm{e}^{(v+1)m_X((1-\alpha)t)}]$ have analytical expressions. However, Proposition 2.1 implies that both of them have closed-form Laplace transforms w.r.t. t, namely $\mathcal{L}_M(s)$ and $\mathcal{L}_m(s)$. Accordingly, in principle we can price fixed-strike quantile options and calculate the two Greeks by applying the Laplace inversion algorithm twice. A rough pricing and hedging algorithm is given as follows.

Step 1. Evaluate $\mathrm{E}[\mathrm{e}^{(v+1)M_X(\alpha t)}]$ and $\mathrm{E}[\mathrm{e}^{(v+1)m_X((1-\alpha)t)}]$ by inverting their Laplace transforms numerically. Then we can obtain $\mathcal{L}(v)$, $(v+1)\mathcal{L}(v)/S_0$, and $v(v+1)\mathcal{L}(v)/S_0^2$.

Step 2. Inverting $\mathcal{L}(v)$, $(v+1)\mathcal{L}(v)/S_0$, and $v(v+1)\mathcal{L}(v)/S_0^2$, and then multiplying the results by e^{-rt} yields $C_\alpha(S_0, K, t)$, $\Delta(C_\alpha(S_0, K, t))$, and $\Gamma(C_\alpha(S_0, K, t))$, respectively.

It is worth mentioning here that by 'applying the Laplace inversion algorithm twice' we mean that a single Laplace inversion algorithm is applied in both step 1 and step 2. This greatly differs from the so-called 'double Laplace inversion'. Specifically, if the closed-form expression of $\int_{-\infty}^{+\infty} \int_0^{+\infty} \mathrm{e}^{-vk} \mathrm{e}^{-wt} C_\alpha^*(S_0, k, t)\, \mathrm{d}t\, \mathrm{d}k$ is available, it is called the double Laplace transform of $C_\alpha^*(S_0, k, t)$ w.r.t. k and t. Then the double Laplace inversion algorithm applies (see [11]). However, in our case, a closed-form expression of the double Laplace transform of $C_\alpha^*(S_0, k, t)$ is not available. So we attempt to evaluate $C_\alpha^*(S_0, k, t)$ by inverting its single Laplace transform $\mathcal{L}(v)$. But

$$\mathcal{L}(v) = \frac{S_0^{v+1}}{v(v+1)X^v} \mathrm{E}[\mathrm{e}^{(v+1)M_X(\alpha t)}]\mathrm{E}[\mathrm{e}^{(v+1)m_X((1-\alpha)t)}]$$

has no closed-form expression, either. To evaluate $\mathcal{L}(v)$, we need to invert the closed-form Laplace transforms of $\mathrm{E}[\mathrm{e}^{(v+1)M_X(\alpha t)}]$ and $\mathrm{E}[\mathrm{e}^{(v+1)m_X((1-\alpha)t)}]$. To summarize, the 'whole inversion' should be divided into two steps, each of which uses the single Laplace inversion. This is the crucial difference from 'the double Laplace inversion', and we call it 'Laplace inversion twice'.

Nonetheless, when implementing the above algorithm using the Euler inversion algorithm, we encounter some difficulty, primarily because the Euler inversion algorithm applies for only the real original functions and meanwhile the inversion formula involves Laplace transforms in the complex domain. As a result, to invert $\mathcal{L}(v)$ in step 2, we need values of $\mathcal{L}(v)$ for complex v. This means that in step 1, we need to evaluate $\mathrm{E}[\mathrm{e}^{(v+1)M_X(\alpha t)}]$ and $\mathrm{E}[\mathrm{e}^{(v+1)m_X((1-\alpha)t)}]$ for complex v by inverting their Laplace transforms w.r.t. t. If we apply the Euler inversion algorithm in step 1 directly, it will fail in that this is equivalent to applying the Euler inversion algorithm in the case of complex original functions. To circumvent this difficulty, we evaluate

the real parts and the imaginary parts of $\mathrm{E}[\mathrm{e}^{(v+1)M_X(\alpha t)}]$ and $\mathrm{E}[\mathrm{e}^{(v+1)m_X((1-\alpha)t)}]$ separately. For details, see Section 4.

3.2. Pricing and hedging of floating-strike quantile options

Compared with pricing and hedging of the fixed-strike quantile option, the floating-strike quantile option seems more intractable because its price not only depends on the quantile but also on the terminal asset value. Nevertheless, we can bridge these two issues by transforming the floating-strike option price to the price of a fixed-strike option by virtue of Girsanov's theorem for jump diffusion processes. This idea stems from Leung and Kwok [26], who established a relationship between fixed- and floating-strike quantile option prices under the BSM.

In this part we just provide some new notation and main results. For the details of the proof, see Appendix B. To facilitate the derivation, we consider a quantile option, where the underlying asset has a dividend with rate q. Note that this slight modification does not affect essentially the correctness of Proposition 2.1 and Theorem 3.1. Rewrite the fixed- and floating-strike quantile option prices with maturity T as

$$C_\alpha(S_0, K, T, \mathscr{S}) = \mathrm{e}^{-rT}\,\mathrm{E}[(Q(\alpha, T, \mathscr{S}) - K)^+]$$

and

$$P_\alpha(S_0, T, \mathscr{S}) = \mathrm{e}^{-rT}\,\mathrm{E}[(Q(\alpha, T, \mathscr{S}) - S(T))^+],$$

respectively, where $Q(\alpha, t, \mathscr{S})$ is the α-quantile of the underlying asset price process $\mathscr{S}$ starting from the point S_0.

Now we introduce two independent processes $\mathscr{S}$ and $\bar{\mathscr{S}}$. The former is defined as

$$\mathscr{S} := \left\{ S(t) := S_0 \exp\left(\mu t + \sigma W(t) + \sum_{i=1}^{N(t)} Y_i \right) : t \geq 0 \right\},$$

where all the parameters are the same as those in (2.1) except that $\mu := r - q - \sigma^2/2 - \lambda\zeta$ and $\eta_i > 2$ for any $i = 1, 2, \ldots, m$. The latter is given by

$$\bar{\mathscr{S}} := \left\{ \bar{S}(t) := S_0 \exp\left(\bar{\mu} t + \sigma \overline{W}(t) + \sum_{i=1}^{\widetilde{N}(t)} \overline{Y}_i \right) : t \geq 0 \right\},$$

where $\bar{\mu} = \bar{r} - \bar{q} - \sigma^2/2 - \widetilde{\lambda}\bar{\zeta}$, $\bar{r} = q$, $\bar{q} = r - \lambda\zeta - \widetilde{\lambda}\bar{\zeta}$, $\bar{\zeta} = \mathrm{E}\,\mathrm{e}^{\overline{Y}_1} - 1$, $\{\widetilde{N}(t): t \geq 0\}$ is a Poisson process with rate $\widetilde{\lambda} := \lambda(\zeta + 1)$, $\{\overline{W}(t): t \geq 0\}$ is a standard Brownian motion, and $\{\overline{Y}_i: i = 1, 2, \ldots\}$ is a sequence of i.i.d. hyperexponential random variables with PDF

$$f_{\overline{Y}}(x) = \sum_{i=1}^{n} \bar{p}_i \bar{\eta}_i \mathrm{e}^{-\bar{\eta}_i x} \mathbf{1}_{\{x \geq 0\}} + \sum_{j=1}^{m} \bar{q}_j \bar{\theta}_j \mathrm{e}^{\bar{\theta}_j x} \mathbf{1}_{\{x < 0\}},$$

with

$$\bar{p}_i = \frac{q_i \theta_i}{(\zeta + 1)(\theta_i + 1)} > 0 \quad \text{and} \quad \bar{\eta}_i = \theta_i + 1 > 1 \quad \text{for all } i = 1, \ldots, n,$$

$$\bar{q}_j = \frac{p_j \eta_j}{(\zeta + 1)(\eta_j - 1)} > 0 \quad \text{and} \quad \bar{\theta}_j = \eta_j - 1 > 1 \quad \text{for all } j = 1, \ldots, m.$$

Here $\bar{\theta}_j > 1$ holds for any $j = 1, \ldots, m$ due to the assumption that $\eta_j > 2$ for any $j = 1, \ldots, m$. This guarantees that $\mathrm{E}(\mathrm{e}^{-\overline{Y}_1})$ is finite. Then we have the following theorem.

Theorem 3.2. (Pricing and hedging of floating-strike quantile options.) *With the above notation, the floating-strike quantile option price is*

$$P_\alpha(S_0, T, \mathcal{S}) = C_\alpha(S_0, S_0, T, \bar{\mathcal{S}}) \qquad (3.3)$$

and the two common Greeks $\Delta(P_\alpha(S_0, T, \mathcal{S}))$ *and* $\Gamma(P_\alpha(S_0, T, \mathcal{S}))$ *are given by*

$$\Delta(P_\alpha(S_0, T, \mathcal{S})) := \frac{\partial}{\partial S_0} P_\alpha(S_0, T, \mathcal{S}) = C_\alpha(1, 1, T, \bar{\mathcal{S}})$$

and

$$\Gamma(P_\alpha(S_0, T, \mathcal{S})) := \frac{\partial^2}{\partial S_0^2} P_\alpha(S_0, T, \mathcal{S}) = 0.$$

Proof. See Appendix B.

Theorem 3.2 implies that we can price the floating-strike quantile option by pricing a closely related fixed-strike quantile option. In particular, we can price the European lookback put option at time 0, where the payoff is given by $S_0 e^{M_X(T)} - S(T)$, and which is actually a special case of the floating-strike α-quantile option with $\alpha = 1$.

Remark 3.1. In a recent paper [9] Cai *et al.* investigated pricing and hedging of occupation-time-related options under the DEM, including the fixed-strike quantile options. In comparison, there exist several key differences between our paper and [9]. First, our model is more general and the DEM is only a special case of the HEM. Second, we solve the pricing and hedging problems for both fixed- and floating-strike quantile options, whereas [9] discussed only the fixed-strike case. Third, their pricing method depends on the distribution of the occupation time, which they spent considerable effort deriving. Our approach, however, does not require this technical result.

4. The pricing and hedging algorithm via Euler inversion

In financial applications, numerical inversion of Laplace transforms has become increasingly important for it is always much easier to derive a closed-form expression for the Laplace transform of a derivative price than for the price itself. In this paper we will employ the Euler inversion algorithm to invert Laplace transforms numerically, which was proposed in the one-sided case by Abate and Whitt [1] and was extended to the two-sided case by Petrella [30]. For a survey on comparison of different transform inversion methods applied in asset pricing, we refer the reader to [12].

4.1. The Euler inversion algorithm

When implementing our pricing method proposed in Section 3, we are confronted with two types of Laplace transform. One is one-sided, meaning that the original function is defined on the positive real line, e.g. $\mathcal{L}_M(s)$ and $\mathcal{L}_m(s)$; while the other is two-sided, meaning that the original function is defined on the whole real line, e.g. $\mathcal{L}(v)$.

Suppose that $\hat{f}(s)$ is a two-sided Laplace transform of a nonnegative function $f(t)$ defined on the whole real line $\mathbb{R}$, i.e. $\hat{f}(s) := \int_{-\infty}^{+\infty} e^{-st} f(t)\, dt$. Then we have the following inversion formula (see [30]):

$$f(t) = \frac{e^{A/2}}{2t} \text{Re}\left(\hat{f}\left(\frac{A}{2t}\right)\right) + \frac{e^{A/2}}{t} \sum_{j=1}^{\infty} (-1)^j \text{Re}\left(\hat{f}\left(\frac{A - 2j\pi i}{2t}\right)\right) - e_d. \qquad (4.1)$$

Here Re(z) represents the real part of z, $e_d = e_d^+ + e_d^-$, and

$$e_d^+ = \sum_{j=1}^{+\infty} e^{-jA} f((2j+1)t) \quad \text{and} \quad e_d^- = \sum_{j=-\infty}^{-1} e^{-jA} f((2j+1)t), \qquad (4.2)$$

where A is an arbitrary positive constant used to control the discretization error e_d.

If $\hat{f}(s)$ is a one-sided Laplace transform of a nonnegative function $f(t)$ defined on the positive real line $\mathbb{R}^+$, i.e. $\hat{f}(s) := \int_0^{+\infty} e^{-st} f(t)\, dt$, (4.1) and (4.2) still hold except that e_d^- disappears.

Note that there exist three kinds of parameter involved in the implementation of the Euler inversion algorithm. (i) (n_1, n_2). During the computation, we have to calculate some alternating series of the form $\sum_{i=0}^{\infty} (-1)^i a_i$ in expression (4.1). To accelerate the convergence, we adopt the idea of the Euler transformation, which gives a much faster convergence of the infinite sum (see [1]). More precisely, $\sum_{i=0}^{\infty} (-1)^i a_i$ can be approximated by the finite sum

$$E(m, n) = \sum_{k=0}^{m} \frac{m!}{k!\,(m-k)!} 2^{-m} S_{n+k},$$

where $S_j := \sum_{i=0}^{j} (-1)^i a_i$. Since there are two transform inversions in two steps when pricing fixed-strike quantile options, the Euler transformation is used twice. We use (n_1, m_1) and (n_2, m_2) to express parameters involved in the Euler transformation for Euler inversion w.r.t. the scaled strike k and maturity t, respectively. According to Abate and Whitt's suggestion (see [1]), we set $m_1 = n_1 + 15$ and $m_2 = n_2 + 15$. In practice, we set $n_1 = n_2 = 90$. (ii) A_1 and A_2. These parameters are used to control the discretization error. The empirical setting is $A_1 = A_2 = 18$. (iii) The scaling factor X. In our case, we will select X as $10\,000$.

The selection of the parameters A_1, A_2, and X does not affect the accuracy, but *does* affect the convergence, as shown by the author. This issue will be discussed in detail in Sections 5.2–5.4.

4.2. Calculate $\mathcal{L}(v)$ for complex v via the Euler inversion algorithm

To invert $\mathcal{L}(v)$ numerically via the Euler inversion algorithm, we require values of $\mathcal{L}(v)$ for complex numbers v. Therefore, we need to evaluate $\mathrm{E}[e^{(v+1)M_X(\alpha t)}]$ and $\mathrm{E}[e^{(v+1)m_X((1-\alpha)t)}]$ for complex v. More generally, we first illustrate how to calculate $\mathrm{E}[e^{vM_X(t)}]$ and $\mathrm{E}[e^{vm_X(t)}]$ for complex v by inverting their Laplace transforms $\mathcal{L}_M(s)$ and $\mathcal{L}_m(s)$ numerically. Note that the Euler inversion algorithm applies for only real original functions. To solve this problem, we express $g(v, t) := \mathrm{E}[e^{vM_X(t)}]$ as

$$g(v, t) = g_R(a, b, t) + g_I(a, b, t)\mathrm{i} \quad \text{for } v = a + b\mathrm{i},$$

where $g_R(a, b, t)$ and $g_I(a, b, t)$ represent the real part and imaginary parts of $g(v)$, respectively, and

$$g_R(a, b, t) = \mathrm{E}[e^{aM_X(t)} \cos(bM_X(t))] \quad \text{and} \quad g_I(a, b, t) = \mathrm{E}[e^{aM_X(t)} \sin(bM_X(t))].$$

Then in order to calculate $g(v, t) \equiv \mathrm{E}[e^{vM_X(t)}]$ for complex v, it suffices to evaluate $g_R(a, b, t)$ and $g_I(a, b, t)$ via Euler inversion, both of which are real functions so that the Euler inversion algorithm applies. Denote the Laplace transforms of $g_R(a, b, t)$ and $g_I(a, b, t)$ for a complex number $v = a + b\mathrm{i}$ w.r.t. t by $\mathcal{L}_{MR}(a, b, s)$ and $\mathcal{L}_{MI}(a, b, s)$, respectively. More precisely, for any $s > 0$,

$$\mathcal{L}_{MR}(a, b, s) := \int_0^\infty e^{-st} g_R(a, b, t)\, dt \quad \text{and} \quad \mathcal{L}_{MI}(a, b, s) := \int_0^\infty e^{-st} g_I(a, b, t)\, dt.$$

Their closed-form expressions are derived in the following theorem.

Theorem 4.1. *For any $s > 0$, $v = a + bi$, and $a \in (-\infty, \beta_1)$, we have*

$$\mathcal{L}_{MR}(a, b, s) = \frac{1}{s}\left\{1 + \sum_{l=1}^{m+1}\left[\frac{a(\beta_l - a) - b^2}{(a - \beta_l)^2 + b^2}d_l\right]\right\} \tag{4.3}$$

and

$$\mathcal{L}_{MI}(a, b, s) = \frac{1}{s}\sum_{l=1}^{m+1}\frac{b\beta_l d_l}{(a - \beta_l)^2 + b^2}, \tag{4.4}$$

where $\beta_1, \beta_2, \ldots, \beta_{m+1}$ and $d = (d_1, d_2, \ldots, d_{m+1})^\top$ are the same as in Proposition 2.1.

Proof. The proof is similar to that of Proposition 2.1 of [8] and, thus, is omitted.

Consequently, for complex $v = a + bi$, by inverting $\mathcal{L}_{MR}(a+1, b, \alpha s)$ and $\mathcal{L}_{MI}(a+1, b, \alpha s)$, we can obtain both $g_R(a + 1, b, \alpha t)$ and $g_I(a + 1, b, \alpha t)$, hence getting $\mathrm{E}[\mathrm{e}^{(v+1)M_X(\alpha t)}]$. As for $\mathrm{E}[\mathrm{e}^{(v+1)m_X((1-\alpha)t)}]$, a similar idea applies. In this way, we can evaluate $\mathcal{L}(v)$ for complex v numerically.

4.3. The pricing and hedging algorithm

To summarize, a detailed pricing and hedging algorithm for quantile options under the HEM is given as follows.

Step 1. Evaluate $g_R(a + 1, b, \alpha t)$ and $g_I(a + 1, b, \alpha t)$ by inverting their Laplace transforms $\mathcal{L}_{MR}(a + 1, b, \alpha s)$ and $\mathcal{L}_{MI}(a + 1, b, \alpha s)$ in (4.3) and (4.4), respectively. Thus, we obtain $\mathrm{E}[\mathrm{e}^{(v+1)M_X(\alpha t)}]$ for complex $v = a + bi$.

Step 2. Obtain $\mathrm{E}[\mathrm{e}^{(v+1)m_X((1-\alpha)t)}]$ for complex v in a similar way as in step 1. As a result, we have actually obtained $\mathcal{L}(v)$, $(v + 1)\mathcal{L}(v)/S_0$, and $v(v + 1)\mathcal{L}(v)/S_0^2$ for complex v.

Step 3. Price quantile options and calculate the two Greeks, delta and gamma, by inverting $\mathcal{L}(v)$, $(v + 1)\mathcal{L}(v)/S_0$, and $v(v + 1)\mathcal{L}(v)/S_0^2$, respectively, and by using their values with complex v obtained via step 1 and step 2.

In particular, under the BSM, the pricing and hedging algorithm can be simplified to only one step, i.e. step 3, because $\mathcal{L}(v)$ has the closed-form expression in (3.2).

5. Numerical results

5.1. Calculating prices and Greeks under the HEM

Based on the pricing and hedging algorithm in Section 4.3, Theorem 3.1, Theorem 3.2, and Theorem 4.1, we can price both fixed- and floating-strike quantile options and calculate the associated two Greeks (delta and gamma) under the HEM. Without loss of generality, we focus on a simple case, $m = n = 2$, for the hyperexponential distribution given by (2.2), i.e. both the upward and downward jump size distributions are a mixture of two exponential distributions. The corresponding numerical prices, deltas and gammas (denoted by LL price, LL delta, and LL gamma) of fixed- and floating-strike quantile options are given in Table 1 and Table 2. All the computations are completed on a desktop with an Intel® 2.66 GHz processor. It turns out that all the numerical results stay within the 95% confidence intervals of Monte Carlo simulation estimates (denoted by MC price, MC delta, and MC gamma). Moreover, for the pricing, the averages of absolute values of absolute and relative errors are 0.661 cents and 0.116%, respectively. Therefore, we draw the conclusion that our pricing algorithm is accurate. In addition, the CPU time to produce one LL price (LL delta or LL gamma) is around

TABLE 1: Pricing fixed- and floating-strike quantile options. The default parameters are $\alpha = 0.5$, $r = 0.05$, $\eta_1 = \theta_1 = 30$, $\eta_2 = \theta_2 = 40$, $p_1 = p_2 = 0.3$, $q_1 = q_2 = 0.2$, $S_0 = 100$, $t = 1$, $A_1 = A_2 = 18$, $n_1 = n_2 = 90$, and $X = 10\,000$. The LL price is obtained by using Laplace inversion twice. The MC price is the Monte Carlo simulation estimate obtained by simulating $100\,000$ paths and using $100\,000$ time steps. SE is the associated standard error. AE and RE are the absolute and relative errors between LL price and MC price, respectively.

Pricing fixed-strike quantile options under the HEM							
λ	σ	K	LL price	MC price	SE	AE	RE (%)
1	0.2	90	12.511 58	12.513 55	0.007 22	−0.001 97	−0.016
		100	5.737 06	5.737 99	0.011 54	−0.000 93	−0.016
		110	2.128 64	2.121 84	0.011 22	0.006 80	0.320
1	0.3	90	13.695 27	13.697 02	0.013 23	−0.001 75	−0.013
		100	7.731 21	7.734 64	0.017 20	−0.003 43	−0.044
		110	4.038 86	4.030 32	0.017 58	0.008 54	0.212
3	0.2	90	12.595 88	12.598 49	0.007 76	−0.002 61	−0.021
		100	5.904 13	5.907 02	0.012 08	−0.002 89	−0.049
		110	2.292 06	2.284 97	0.011 86	0.007 09	0.310
3	0.3	90	13.771 24	13.777 66	0.013 57	−0.006 42	−0.047
		100	7.843 86	7.851 46	0.017 54	−0.007 60	−0.097
		110	4.154 15	4.147 03	0.017 96	0.007 12	0.172
Pricing floating-strike quantile options under the HEM							
λ	σ	K	LL price	MC price	SE	AE	RE (%)
1	0.2	—	3.455 66	3.446 20	0.016 69	0.009 46	0.275
	0.3	—	5.523 82	5.508 49	0.024 68	0.015 33	0.278
3	0.2	—	3.629 04	3.615 63	0.017 39	0.013 41	0.371
	0.3	—	5.641 06	5.624 56	0.025 10	0.016 50	0.293

21 seconds, which is practically acceptable and is much less than that of the Monte Carlo simulation (around 25 minutes). So our pricing algorithm is also efficient. In particular, we can price both fixed- and floating-strike quantile options under two important models, the BSM and the DEM, in the same way (note that quantile options under the BSM can be priced more easily via a single Laplace inversion). Furthermore, our algorithm runs very fast under the BSM and DEM (the CPU times to generate one numerical result under the BSM and DEM are around 0.1 seconds and 1.7 seconds, respectively). To save space, we omit the corresponding numerical tables, but they are available on request.

It is worth mentioning that the Monte Carlo simulation estimates listed here, *which serve only as a benchmark*, are obtained via an (almost) plain Monte Carlo simulation scheme along with the variance reduction technique of control variates. For more variance reduction techniques of the Monte Carlo simulation in financial engineering, we refer the reader to the monograph by Glasserman [20].

In addition, Kwok and Lau (see, [25, p. 10]) provided one numerical result (around 9.18, with an associated parameter setting of $\alpha = 0.8$, $r = 0.05$, $\sigma = 0.2$, $S_0 = 100$, $K = 95$, and $t = 0.25$) using a forward shooting grid method, whereas applying our Euler inversion method yields 9.1873. The coincidence also implies the correctness of our method.

TABLE 2: Hedging parameters of fixed- and floating-strike quantile options. The default parameters are $\lambda = 3$, $r = 0.05$, $\eta_1 = \theta_1 = 30$, $\eta_2 = \theta_2 = 40$, $p_1 = p_2 = 0.3$, $q_1 = q_2 = 0.2$, $S_0 = 100$, $t = 1$, $A_1 = A_2 = 18$, $n_1 = n_2 = 90$, and $X = 10\,000$. LL deltas and LL gammas are obtained by using Laplace inversion twice. MC deltas and MC gammas are the Monte Carlo simulation estimates obtained by simulating 100\,000 paths and using 100\,000 time steps. SE is the associated standard error.

		Deltas of fixed-strike quantile options under the HEM					
σ	K	$\alpha = 0.3$			$\alpha = 0.6$		
		LL delta	MC delta	SE	LL delta	MC delta	SE
0.2	90	0.721 19	0.720 03	0.000 77	0.899 53	0.898 99	0.000 70
	100	0.420 80	0.422 19	0.000 97	0.649 66	0.650 52	0.000 97
	110	0.146 37	0.147 24	0.000 91	0.348 85	0.349 56	0.000 97
0.3	90	0.616 53	0.616 51	0.000 80	0.841 06	0.840 73	0.000 80
	100	0.395 35	0.396 68	0.000 96	0.638 39	0.637 67	0.000 96
		Deltas of floating-strike quantile options under the HEM					
σ	K	$\alpha = 0.3$			$\alpha = 0.6$		
		LL delta	MC delta	SE	LL delta	MC delta	SE
0.2	—	0.019 30	0.019 18	0.000 12	0.046 76	0.046 66	0.000 20
0.3	—	0.029 78	0.029 64	0.000 17	0.072 84	0.072 74	0.000 29
		Gammas of fixed-strike quantile options under the HEM					
σ	K	$\alpha = 0.3$			$\alpha = 0.6$		
		LL gamma	MC gamma	SE	LL gamma	MC gamma	SE
0.2	90	0.019 92	0.020 79	0.001 57	0.013 63	0.012 43	0.001 21
	100	0.036 47	0.039 24	0.002 25	0.034 32	0.035 31	0.002 15
	110	0.019 56	0.020 28	0.001 68	0.026 81	0.028 21	0.002 01
0.3	90	0.017 15	0.017 70	0.001 43	0.014 03	0.012 75	0.001 19
	100	0.024 29	0.027 83	0.001 88	0.024 24	0.025 59	0.001 79
	110	0.016 49	0.015 48	0.001 44	0.020 69	0.022 07	0.001 77

5.2. Sensitivity of our numerical algorithm to A_1, A_2, and X

Observe that the Euler inversion algorithm depends on the selection of parameters A_1, A_2, and X, all of which are primarily for discretization error control. As a matter of fact, the algorithm is quite insensitive to changes in A_1, A_2, and X. This property is well illustrated by Figure 1, where the upper three graphs show how the absolute errors between the LL prices and MC prices change as A_1, A_2, and X vary; while the lower three graphs show the corresponding relative errors. Actually, the LL prices keep accurate and stable when these parameters vary in broad regions, i.e. $A_1 \in [15, 45]$, $A_2 \in [15, 45]$, and $X \in [1000, 30\,000]$. The absolute values of associated relative errors between LL prices and MC prices are stable and stay smaller than 0.06%. Consequently, we draw the conclusion that our pricing algorithm is stable and, thus, reliable.

5.3. Convergence and computational cost of our numerical algorithm

Recall that our numerical algorithm involves four algorithm parameters, n_1 (and n_2, typically we select $n_2 = n_1$ in practice), A_1, A_2, and X. As discussed in Section 4.1, n_1 (and n_2) is
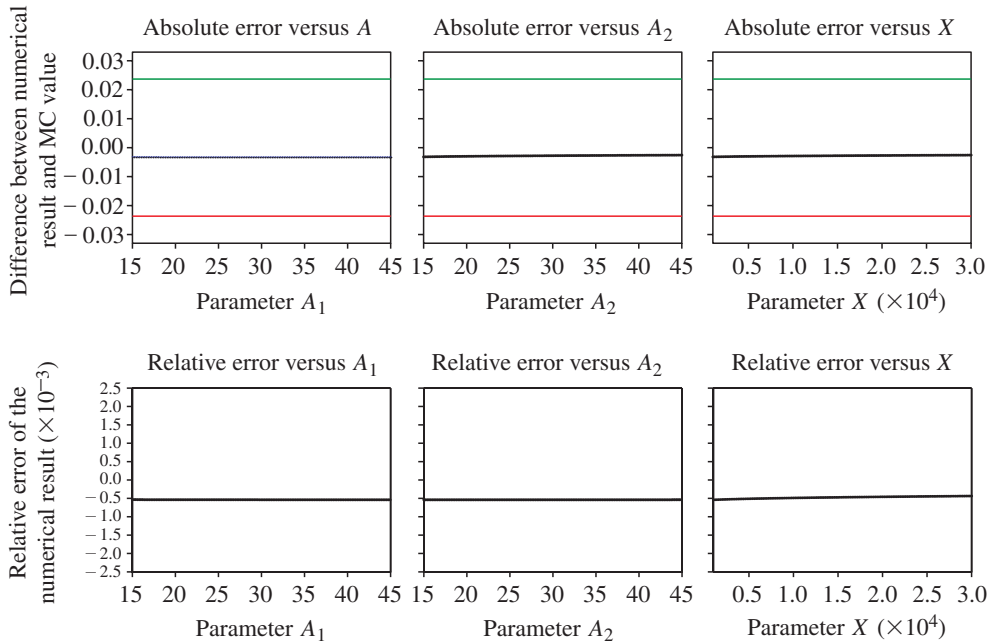
FIGURE 1: How the numerical results (LL prices) change as A_1, A_2, and X vary. The parameter setting is $\alpha = 0.5$, $r = 0.05$, $\sigma = 0.2$, $\lambda = 3$, $\eta_1 = \theta_1 = 30$, $\eta_2 = \theta_2 = 40$, $p_1 = p_2 = 0.3$, $q_1 = q_2 = 0.2$, $S_0 = 100$, $t = 1$, and $n_1 = n_2 = 90$. *Upper-left graph*: absolute error versus A_1, where $A_2 = 18$ and $X = 10\,000$. *Upper-middle graph*: absolute error versus A_2, where $A_1 = 18$ and $X = 10\,000$. *Upper-right graph*: absolute error versus X, where $A_1 = 18$ and $A_2 = 18$. The lower three graphs show how the corresponding relative errors change.

related to the approximation to the infinite series in the inversion formula (4.1) by some finite sum called the Euler transformation (see [1]). More precisely, applying the Euler transformation to accelerate the rate of the convergence of a series, we approximate the infinite series of the form $\sum_{i=0}^{\infty}(-1)^i a_i$ in the inversion formula (4.1) by the finite sum

$$E(m_1, n_1) = \sum_{k=0}^{m_1} \frac{m_1!}{k!(m_1 - k)!} 2^{-m_1} S_{n_1+k},$$

where $m_1 = n_1 + 15$ (suggested by Abate and Whitt [1]) and $S_j := \sum_{i=0}^{j}(-1)^i a_i$ for $j = 0, 1, \ldots$. It is easily seen that the finite sum $E(m_1, n_1)$ involves only the first $m_1 + n_1 = 2n_1 + 15$ terms of the series. Therefore, the larger n_1, the more accurate the approximation. As n_1 goes to ∞, the approximation converges to the sum of the infinite series.

In this section we intend to study how our numerical algorithm converges as n_1 increases, given A_1, A_2, and X. For ease of exposition, we denote by $p(n_1)$ the numerical quantile option price obtained via our numerical algorithm with parameter n_1. Let n_1 increase from 15 with an increment of 5, i.e. $n_1 = 15, 20, 25, 30, \ldots$. It is worth noting that we do not know the true option price, i.e. the limit of the numerical approximation as n_1 goes to ∞. Alternatively, we may use $|p(n_1 + 5) - p(n_1)|$ to measure the convergence, and say that the numerical approximation is sufficiently close to its limit when

$$|p(n_1 + 5) - p(n_1)| < 10^{-4}. \tag{5.1}$$

TABLE 3: How the numerical prices $p(n_1)$ converge and how the CPU times (in seconds) change as n_1 increases. The default parameters are $\alpha = 0.5$, $r = 0.05$, $\eta_1 = \theta_1 = 30$, $\eta_2 = \theta_2 = 40$, $p_1 = p_2 = 0.3$, $q_1 = q_2 = 0.2$, $S_0 = 100$, $t = 1$, $A_1 = A_2 = 18$, and $X = 10\,000$.

| n_1	$p(n_1)$	$\lvert p(n_1+5)-p(n_1)\rvert$	CPU time	n_1	$p(n_1)$	$\lvert p(n_1+5)-p(n_1)\rvert$	CPU time
20	5.921 42	0.007 252	1.73	115	5.903 96	0.000 020	31.97
25	5.914 17	0.003 769	2.36	120	5.903 94	0.000 017	34.56
30	5.910 40	0.002 146	3.11	125	5.903 92	0.000 014	37.16
35	5.908 26	0.001 310	3.97	130	5.903 91	0.000 012	40.02
40	5.906 95	0.000 844	4.98	135	5.903 90	0.000 011	43.08
45	5.906 10	0.000 568	6.05	140	5.903 89	0.000 009	46.11
50	5.905 54	0.000 397	7.19	145	5.903 88	0.000 008	49.36
55	5.905 14	0.000 285	8.48	150	5.903 87	0.000 007	52.55
60	5.904 85	0.000 210	9.86	155	5.903 86	0.000 006	56.11
65	5.904 64	0.000 158	11.34	160	5.903 86	0.000 006	59.73
70	5.904 48	0.000 121	12.98	165	5.903 85	0.000 005	63.16
75	5.904 36	0.000 095	14.67	170	5.903 84	0.000 004	67.00
80	5.904 27	0.000 075	16.48	175	5.903 84	0.000 004	71.02
85	5.904 20	0.000 060	18.41	180	5.903 84	0.000 004	75.02
90	5.904 13	0.000 049	20.39	185	5.903 83	0.000 003	78.97
95	5.904 08	0.000 040	22.50	190	5.903 83	0.000 003	82.81
100	5.904 04	0.000 033	24.97	195	5.903 83	0.000 003	87.39
105	5.904 01	0.000 028	27.02	200	5.903 82	—	91.80
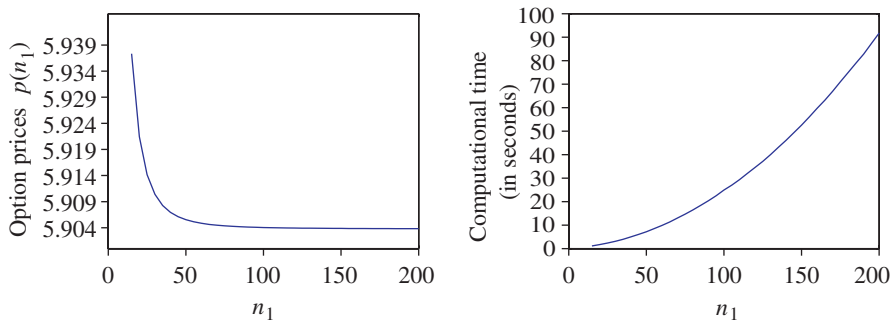
FIGURE 2: The left panel and the right panel illustrate how the numerical prices converge and how the computational times change as $n_1(= n_2)$ increases, respectively. We can see that the numerical prices converge quite fast as n_1 increases. The parameter setting is $\alpha = 0.5$, $r = 0.05$, $\sigma = 0.2$, $\lambda = 3$, $\eta_1 = \theta_1 = 30$, $\eta_2 = \theta_2 = 40$, $p_1 = p_2 = 0.3$, $q_1 = q_2 = 0.2$, $S_0 = 100$, $t = 1$, $A_1 = A_2 = 18$, and $X = 10\,000$.

It turns out that the n_1s that satisfy (5.1) can guarantee three-digit accuracy of our numerical prices.

The results of Table 3 demonstrate how the numerical prices $p(n_1)$ converge as n_1 increases (see also the left panel of Figure 2). It can be seen that when $n_1 \geq 75$, we have $\lvert p(n_1 + 5) - p(n_1)\rvert < 10^{-4}$. Furthermore, this can guarantee at least three-digit accuracy (5.904) for our numerical prices if we round them off to three decimal places. This accuracy is acceptable in practice because of the bid-ask spreads. In order to be safe, we select $n_1 = 90$ when implementing the algorithm in our numerical part (Section 5.1). In addition, the results of

Table 3 also demonstrate how the CPU times change as n_1 increases (see also the right panel of Figure 2). When $n_1 = 90$, the corresponding CPU time is around 21 seconds and practically acceptable.

Note that the above numerical experiments are conducted when $A_1 = 18$, $A_2 = 18$, and $X = 10\,000$ are fixed. However, the convergence speed of our numerical algorithm may also depend on selection of these three algorithm parameters. This issue will be investigated in Section 5.4.

5.4. Effect of A_1, A_2, and X on the convergence speed of our numerical algorithm

To study the effect of the selection of the three parameters A_1, A_2, and X on the convergence speed of our numerical algorithm, we define $N^*(A_1, A_2, X)$ for given A_1, A_2, and X as

$$N^*(A_1, A_2, X) := \min\{n_1 : |p(n_1 + 5) - p(n_1)| < 10^{-4} \text{ and } n_1 = 15, 20, 25, \ldots\}.$$

Note that the smaller $N^*(A_1, A_2, X)$, the faster the convergence. Accordingly, $N^*(A_1, A_2, X)$ may be used to indicate the convergence speed corresponding to the parameter selection, A_1, A_2, and X. As discussed in Section 5.3, the n_1s that satisfy $|p(n_1 + 5) - p(n_1)| < 10^{-4}$ can typically achieve at least three-digit accuracy for our numerical prices if we round them off to three decimal places. This accuracy is acceptable in practice because of the bid-ask spreads.

By plotting $N^*(A_1, A_2, X)$ for various A_1, A_2, and X, Figure 3 illustrates how these three parameters influence the convergence speed of our numerical algorithm. The upper three graphs
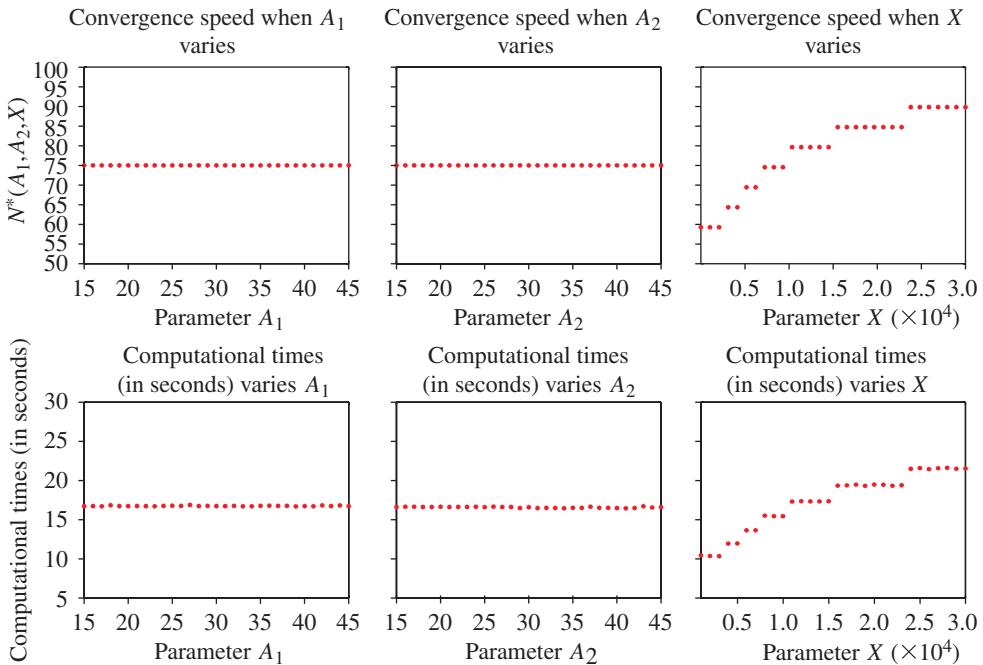

FIGURE 3: The effect of the selection of the three parameters A_1, A_2, and X on the convergence speed of our numerical algorithm. The parameter setting is $\alpha = 0.5$, $r = 0.05$, $\sigma = 0.2$, $\lambda = 3$, $\eta_1 = \theta_1 = 30$, $\eta_2 = \theta_2 = 40$, $p_1 = p_2 = 0.3$, $q_1 = q_2 = 0.2$, $S_0 = 100$, and $t = 1$. *Upper-left graph*: $N^*(A_1, A_2, X)$ versus A_1 when $A_2 = 18$ and $X = 10\,000$. *Upper-middle graph*: $N^*(A_1, A_2, X)$ versus A_2 when $A_1 = 18$ and $X = 10\,000$. *Upper-right graph*: $N^*(A_1, A_2, X)$ versus X when $A_1 = 18$ and $A_2 = 18$. The lower three graphs show how the corresponding computational times change.

show how $N^*(A_1, A_2, X)$ changes when A_1, A_2, and X vary, respectively, whereas the lower three exhibit the corresponding computational times. We can see that the convergence speed of our numerical algorithm seems insensitive to the selection of A_1 and A_2 because broad regions of A_1 and A_2 ($A_1 \in [15, 45]$, $A_2 \in [15, 45]$) can guarantee the same $N^*(A_1, A_2, X)$ ($= 75$). In contrast, the selection of parameter X has a larger effect on the convergence speed. The upper-right graph demonstrates that a larger X tends to result in a larger $N^*(A_1, A_2, X)$, i.e. a slower convergence. However, a broad region of X ($X \in [1000, 30\,000]$) can guarantee $N^*(A_1, A_2, X) \leq 90$. Recall that to be safe, we select $n_1 = 90$ when implementing the numerical algorithm in our numerical part (Section 5.1). Figure 3 indicates that this selection of n_1 is quite good because it can guarantee $|p(n_1 + 5) - p(n_1)| \leq 10^{-4}$ for broad regions of A_1, A_2, and X ($A_1 \in [15, 45]$, $A_2 \in [15, 45]$, and $X \in [1000, 30\,000]$).

Appendix A. Proof of Theorem 3.1

Result (3.1) can be derived as follows:

$$
\begin{aligned}
\mathcal{L}(v) &= \int_{-\infty}^{+\infty} e^{-vk} X \, \mathrm{E}\left[\left(\frac{S_0}{X} e^{Q(\alpha, t, \mathcal{X})} - e^{-k}\right)^+\right] dk \\
&= X \, \mathrm{E}\left[\int_{-\infty}^{+\infty} e^{-vk} \left[\left(\frac{S_0}{X} e^{Q(\alpha, t, \mathcal{X})} - e^{-k}\right)^+\right] dk\right] \\
&= X \, \mathrm{E}\left[\int_{-\log(S_0/X) - Q(\alpha, t, \mathcal{X})}^{+\infty} e^{-vk} \left(\frac{S_0}{X} e^{Q(\alpha, t, \mathcal{X})} - e^{-k}\right) dk\right] \\
&= \frac{S_0^{v+1}}{v(v+1)X^v} \, \mathrm{E}[e^{(v+1)Q(\alpha, t, \mathcal{X})}].
\end{aligned}
$$

In the light of Proposition 2.2, we have

$$
\mathrm{E}[e^{(v+1)Q(\alpha, t, \mathcal{X})}] = \mathrm{E}[e^{(v+1)M_{\mathcal{X}}(\alpha t)}] \mathrm{E}[e^{(v+1)m_{\mathcal{X}}((1-\alpha)t)}].
$$

Then (3.1) follows immediately. Note that, under the BSM, the moment generating function of the running maximum of the drifted Brownian motion during a period can be expressed explicitly with complementary error functions (or error functions). By slightly modifying the formula on page 250 of [5], we can obtain (3.2) easily. Finally, the two Greeks can be obtained by interchanging derivatives and integrals based on Theorem A.12 of [31, pp. 203–204].

Appendix B. Proof of Theorem 3.2

Note that the floating-strike α-quantile option price can be rewritten as

$$
\begin{aligned}
P_\alpha(S_0, T, \mathscr{S}) &= e^{-rT} \, \mathrm{E}[(Q(\alpha, T, \mathscr{S}) - S(T))^+] \\
&= \mathrm{E}\left[\frac{S(T)}{S_0} e^{-rT}\left(\frac{S_0}{S(T)} Q(\alpha, T, \mathscr{S}) - S_0\right)^+\right].
\end{aligned}
\tag{B.1}
$$

Consider introducing a new measure $\widetilde{\mathrm{P}}$ defined as

$$
\left.\frac{d\widetilde{\mathrm{P}}}{d\mathrm{P}}\right|_{t=T} = \frac{S(T)}{S_0} e^{-(r-q)T}.
$$

Then according to Girsanov's theorem for jump diffusion processes (see [32]), we conclude that, under the new measure $\widetilde{P}$, $\{\widetilde{W}(t) := W(t) - \sigma t : 0 \leq t \leq T\}$ becomes a standard Brownian motion, and the original return process

$$X(t) = \left(r - q - \frac{\sigma^2}{2} - \lambda\zeta\right)t + \sigma W(t) + \sum_{i=1}^{N(t)} Y_i$$

$$= \left(r - q + \frac{\sigma^2}{2} - \lambda\zeta\right)t + \sigma \widetilde{W}(t) + \sum_{i=1}^{\widetilde{N}(t)} \widetilde{Y}_i$$

is a new hyperexponential jump diffusion process, where $\{\widetilde{N}(t) : t \geq 0\}$ is a Poisson process with rate $\widetilde{\lambda} = \lambda \, E[e^Y] = \lambda(\zeta + 1)$, and $\{\widetilde{Y}_i : i = 1, 2, \ldots\}$ is also a sequence of i.i.d. hyperexponential random variables with PDF

$$f_{\widetilde{Y}}(x) = f_Y(x) \frac{e^x}{E[e^Y]}$$

$$= \sum_{i=1}^{m} \frac{p_i \eta_i}{(\zeta + 1)(\eta_i - 1)} (\eta_i - 1) e^{-(\eta_i - 1)x} \mathbf{1}_{\{x \geq 0\}}$$

$$+ \sum_{j=1}^{n} \frac{q_j \theta_j}{(\zeta + 1)(\theta_j + 1)} (\theta_j + 1) e^{(\theta_j + 1)x} \mathbf{1}_{\{x < 0\}}$$

$$=: \sum_{i=1}^{n} \widetilde{p}_i \widetilde{\eta}_i e^{-\widetilde{\eta}_i x} \mathbf{1}_{\{x \geq 0\}} + \sum_{j=1}^{m} \widetilde{q}_j \widetilde{\theta}_j e^{\widetilde{\theta}_j x} \mathbf{1}_{\{x < 0\}}.$$

Here

$$\widetilde{p}_i := \frac{p_i \eta_i}{(\zeta + 1)(\eta_i - 1)} > 0 \quad \text{and} \quad \widetilde{\eta}_i := \eta_i - 1 > 1 \quad \text{for all } i = 1, \ldots, m,$$

$$\widetilde{q}_j := \frac{q_j \theta_j}{(\zeta + 1)(\theta_j + 1)} > 0 \quad \text{and} \quad \widetilde{\theta}_j := \theta_j + 1 > 1 \quad \text{for all } j = 1, \ldots, n.$$

By the change of measure, (B.1) is reduced to

$$P_\alpha(S_0, T, \mathscr{S}) = e^{-qT} \widetilde{E}\left[\left(\frac{S_0}{S(T)} Q(\alpha, T, \mathscr{S}) - S_0\right)^+\right]. \tag{B.2}$$

A close scrutiny of $S_0 Q(\alpha, T, \mathscr{S})/S(T)$ (see [16] or [26]) results in

$$\frac{S_0}{S(T)} Q(\alpha, T, \mathscr{S}) = \frac{S_0}{S(T)} \inf\left\{x \in \mathbb{R} : \int_0^T \mathbf{1}_{\{S(t) \leq x\}} \, dt > \alpha T\right\}$$

$$= \inf\left\{\frac{S_0}{S(T)} x \in \mathbb{R} : \int_0^T \mathbf{1}_{\{S_0 S(t)/S(T) \leq S_0 x/S(T)\}} \, dt > \alpha T\right\}$$

$$= \inf\left\{z \in \mathbb{R} : \int_0^T \mathbf{1}_{\{S_0 S(t)/S(T) \leq z\}} \, dt > \alpha T\right\}. \tag{B.3}$$

Note that, for any $t \in [0, T]$,

$$\frac{S_0}{S(T)} S(t) = S_0 \exp\left(\left(r - q + \frac{\sigma^2}{2} - \lambda\zeta\right)(t - T) + \sigma(\widetilde{W}(t) - \widetilde{W}(T)) - \sum_{i=\widetilde{N}(t)+1}^{\widetilde{N}(T)} \widetilde{Y}_i\right)$$

$$= S_0 \exp\left(\left(q - r - \frac{\sigma^2}{2} + \lambda\zeta\right)(T - t) + \sigma[(-\widetilde{W}(T)) - (-\widetilde{W}(t))]\right.$$

$$\left. + \sum_{i=\widetilde{N}(t)+1}^{\widetilde{N}(T)} (-\widetilde{Y}_i)\right).$$

Introduce a new standard Brownian motion $\{\overline{W}(t) := -\widetilde{W}(t) : 0 \leq t \leq T\}$, and define $\overline{Y}_i := -\widetilde{Y}_i$ and $\bar{S}(t) := S_0 \exp(\bar{\mu}t + \sigma\overline{W}(t) + \sum_{i=1}^{\widetilde{N}(t)} \overline{Y}_i)$, where $\bar{\mu} := \bar{r} - \bar{q} - \sigma^2/2 - \widetilde{\lambda}\bar{\zeta}$, $\bar{r} := q$, $\bar{q} := r - \lambda\zeta - \widetilde{\lambda}\bar{\zeta}$, and $\bar{\zeta} := \mathrm{E}\,e^{\overline{Y}} - 1$. Then we claim that, under the new measure $\widetilde{\mathrm{P}}$, the following two processes have the same distribution:

$$\left\{\frac{S_0}{S(T)} S(t) : t \in [0, T]\right\} \overset{\mathrm{D}}{=} \{\bar{S}(T - t) : t \in [0, T]\}. \tag{B.4}$$

Consequently, we know from (B.3) and (B.4) that, under the new measure $\widetilde{\mathrm{P}}$,

$$\frac{S_0}{S(t)} Q(\alpha, T, \mathcal{S}) = \inf\left\{z \in \mathbb{R} : \int_0^T \mathbf{1}_{\{SS(t)/S(T)\leq z\}}\, \mathrm{d}t > \alpha T\right\}$$

$$\overset{\mathrm{D}}{=} \inf\left\{z \in \mathbb{R} : \int_0^T \mathbf{1}_{\{\bar{S}(T-t)\leq z\}}\, \mathrm{d}t > \alpha T\right\}$$

$$= \inf\left\{z \in \mathbb{R} : \int_0^T \mathbf{1}_{\{\bar{S}(t)\leq z\}}\, \mathrm{d}t > \alpha T\right\}$$

$$= Q(\alpha, T, \bar{\mathcal{S}}). \tag{B.5}$$

From (B.2) and (B.5), (3.3) follows immediately. For the two Greeks, noting that

$$P_\alpha(S_0, T, \mathcal{S}) = \mathrm{e}^{-rT}\, \mathrm{E}[(Q(\alpha, T, \mathcal{S}) - S(T))^+] = \mathrm{e}^{-rT}\, \mathrm{E}[(\mathrm{e}^{Q(\alpha, T, \mathcal{X})} - \mathrm{e}^{X(T)})^+]S_0,$$

we easily obtain

$$\Gamma(P_\alpha(S_0, T, \mathcal{S})) = 0$$

and

$$\Delta(P_\alpha(S_0, T, \mathcal{S})) = \mathrm{e}^{-rT}\, \mathrm{E}[(\mathrm{e}^{Q(\alpha, T, \mathcal{X})} - \mathrm{e}^{X(T)})^+] = P_\alpha(1, T, \mathcal{S}) = C_\alpha(1, 1, T, \bar{\mathcal{S}}).$$

The proof is completed.

Acknowledgements

References

[1] ABATE, J. AND WHITT, W. (1992). The Fourier-series method for inverting transforms of probability distributions. *Queueing Systems* **10,** 5–87.

[2] AKAHORI, J. (1995). Some formulae for a new type of path-dependent option. *Ann. Appl. Prob.* **5,** 383–388.

[3] ASMUSSEN, S., AVRAM, F. AND PISTORIUS, M. R. (2004). Russian and American put options under exponential phase-type Lévy models. *Stoch. Process. Appl.* **109,** 79–111.

[4] BERTOIN, J., CHAUMONT, L. AND YOR, M. (1997). Two chain transformations and their applications to quantiles. *J. Appl. Prob.* **34,** 882–897.

[5] BORODIN, A. N. AND SALMINEN P. (2002). *Handbook of Brownian Motion—Facts and Formulae*, 2nd edn. Birkhäuser, Basel.

[6] BROADIE, M. AND DETEMPLE, J. B. (2004). Option pricing: valuation models and applications. *Manag. Sci.* **50,** 1145–1177.

[7] CAI, N. (2009). On first passage times of a hyper-exponential jump diffusion process. *Operat. Res. Lett.* **37,** 127–134.

[8] CAI, N. AND KOU, S. G. (2011). Option pricing under a mixed-exponential jump diffusion model. To appear in *Mamag. Sci.*

[9] CAI, N., CHEN, N. AND WAN, X. (2010). Occupation times of jump-diffusion processes with double exponential jumps and the pricing of options. *Math. Operat. Res.* **35,** 412–437.

[10] CARR, P. AND MADAN, D. B. (1999). Option valuation using the fast Fourier transform. *J. Comput. Finance* **2,** 61–73.

[11] CHOUDHURY, G. L., LUCANTONI, D. M. AND WHITT, W. (1994). Multidimensional transform inversion with applications to the transient M/G/1 queue. *Ann. Appl. Prob.* **4,** 719–740.

[12] CRADDOCK, M., HEATH, D. AND PLATEN, E. (2000). Numerical inversion of Laplace transforms: a survey of techniques with applications to derivative pricing. *J. Comput. Finance* **4,** 57–81.

[13] DASSIOS, A. (1995). The distribution of the quantile of a Brownian motion with drift and the pricing of related path-dependent options. *Ann. Appl. Prob.* **5,** 389–398.

[14] DASSIOS, A. (1996). Sample quantiles of stochastic processes with stationary and independent increments. *Ann. Appl. Prob.* **6,** 1041–1043.

[15] DAVYDOV, D. AND LINETSKY, V. (2001). Structuring, pricing and hedging double barrier step options. *J. Comput. Finance* **5,** 55–87.

[16] DETEMPLE, J. (2001). American options: symmetry properties. In *Option Pricing, Interest Rates and Risk Management*, eds E. Jouini, J. Cvitanic and M. Musiela, Cambridge University Press, pp. 67–104.

[17] EMBRECHTS, P., ROGERS, L. C. G. AND YOR, M. (1995). A proof of Dassios' representation of the α-quantile of Brownian motion with drift. *Ann. Appl. Prob.* **5,** 757–767.

[18] FUSAI, G. (2000). Corridor options and arc-sine law. *Ann. Appl. Prob.* **10,** 634–663.

[19] FUSAI, G. AND TAGLIANI, A. (2001). Pricing of occupation time derivatives: continuous and discrete monitoring. *J. Comput. Finance* **5,** 1–37.

[20] GLASSERMAN, P. (2000). *Monte Carlo Methods in Financial Engineering*. Springer, New York.

[21] HUGONNIER, J. (1999). The Feynman-Kac formula and pricing occupation time derivatives. *Internat. J. Theoret. Appl. Finance* **2,** 153–178.

[22] JEANNIN, M. AND PISTORIUS, M. (2010). A transform approach to compute prices and Greeks of barrier options driven by a class of Lévy processes. *Quant. Finance* **10,** 629–644.

[23] KOU, S. G. (2002). A jump-diffusion model for option pricing. *Manag. Sci.* **48,** 1086–1101.

[24] KWOK, Y. K. (1998). *Mathematical Models of Financial Derivatives*. Springer, Singapore.

[25] KWOK, Y. K. AND LAU, K. W. (2001). Pricing algorithms for options with exotic path-dependence. *J. Derivatives* **9,** 23–38.

[26] LEUNG, K. S. AND KWOK, Y. K. (2007). Distribution of occupation times for constant elasticity of variance diffusion and the pricing of α-quantile options. *Quant. Finance* **7,** 87–94.

[27] LINETSKY, V. (1999). Step options. *Math. Finance* **9,** 55–96.

[28] MIURA, R. (1992). A note on look-back options based on order statistics. *Hitotsubashi J. Commerce Manag.* **27,** 15–28.

[29] PECHTL, A. (1999). Some applications of occupation times of Brownian motion with drift in mathematical finance. *J. Appl. Math. Decision Sci.* **3,** 63–73.

[30] PETRELLA, G. (2004). An extension of the Euler Laplace transform inversion algorithm with applications in option pricing. *Operat. Res. Lett.* **32,** 380–389.
[31] SCHIFF, J. L. (1999). *The Laplace Transform*. Springer, New York.
[32] SCHORODER, M. (1999). Changes of numeraire for pricing futures, forwards, and options. *Rev. Financial Studies* **12,** 1143–1163.
[33] SHREVE, S. E. (2004). *Stochastic Calculus for Finance. II*. Springer, New York.
[34] YOR, M. (1995). The distribution of Brownian quantiles. *J. Appl. Prob.* **32,** 405–416.